

03,10

## Threshold effects in the energy spectrum of quasi-two-dimensional electrons of the accumulation layer

© A.Ya. Shul'man, D.V. Posvyanskii

Kotelnikov Institute of Radio Engineering and Electronics, Russian Academy of Sciences,  
Moscow, Russia

E-mail: ash@cplire.ru

Received April 26, 2024

Revised April 26, 2024

Accepted May 3, 2024

We consider the problem of determining the threshold values of the electric field  $F$  at which new size-quantized subbands appear in the accumulation layer on the surface of an  $n$ -type semiconductor. The difficulties of such determination in experimental and computational works presented in the literature are discussed. An explanation of the available facts is proposed as a manifestation of the quadratic dependence of the energy  $E$  of the shallow level on the depth of the potential well near the appearance threshold. Formulae of threshold dependence  $E(F)$  for the case of parabolic conduction band in the bulk of semiconductor are obtained. The possibility of application of the threshold approximation not only to the main, but also to the excited subbands is shown. In the case of non-parabolic conduction band, the threshold character in dependence of the size-quantized level energy on quasimomentum along the surface is considered. Numerical calculations of two-dimensional spectra under the conditions of the appearance of the main subband, the first and the second excited ones have been performed with  $n$ -InAs parameters and analyzed by means of the derived expressions for the threshold behavior. A method to determine the threshold of a subband appearance from available data in the region above the threshold is proposed. An instability of the self-consistent solution of the system from the Poisson equation and the effective mass equation in the case of the second excited subband is observed and investigated. Arguments are presented in favor of interpreting this instability as evidence of the formation of two-dimensional valence-type subbands with negative mass in the accumulation layer. We discuss a possible connection between the appearance of such a spectrum in the potential well, the deep of which is comparable to the bandgap, and L.V. Keldysh's assumption about the origin of the amphotericity of impurities that create deep levels in the semiconductor bandgap.

**Keywords:** semiconductors, low-dimensional structures, accumulation layer, two-band Kane model, effective mass equation, threshold phenomena in two-dimensional spectrum.

DOI: 10.61011/PSS.2024.06.58709.109

### 1. Introduction

When creating an accumulation layer on the surface of an  $n$ -type semiconductor in a metal-insulator-semiconductor structure, the number of occupied size-quantized subbands is determined experimentally from the dependence of the surface density  $n_s$  of electrons on the potential  $V_g$  of the metal gate. When a new subband appears, the number of electrons in it is relatively small and poorly determined. Therefore, the value of  $V_{gc}$  when a new subband appears is found by linear extrapolation of the measured dependence of  $n_s(V_g)$  to zero (see for example [1], Figures 3 and 9). In this case, it is discovered that quasi-two-dimensional electrons exist at  $V_g < V_{gc}$ . There was no generally accepted explanation for this observation.

When an electron accumulation layer near the surface is formed by the adsorption of positive ions due to the formation of a band-bending region, the number of size-quantized subbands is determined either experimentally by photoelectron spectroscopy, which is difficult, or by solving the effective mass equation. In the latter case for electrons with a nonparabolic conduction band, the energy of levels

size-quantized normal to the surface depends on the lateral component of the quasimomentum  $k_{\parallel}^2$  along the surface. In case of band bending corresponding to the beginning of the separation of the size-quantized subband from the continuous spectrum, the calculation of the two-dimensional energy spectrum showed the existence of a two-dimensional subband, the spectrum of which began at a certain critical value  $k_{\parallel c} > 0$  [2]. As an explanation, a hypothesis was put forward about the possible existence of size-quantized subbands, their minimum located at  $k_{\parallel c} \neq 0$ .

However, in both cases described, when a new subband appears, its minimum will necessarily be located near the boundary of the continuous spectrum, and it should correspond to a small binding energy. In such cases, one should expect a quadratic dependence of the energy spectrum on the depth of the potential well, characteristic of the threshold effect ([3] Ch. I, § 2). This makes it difficult to detect the shallow state at an early stage deepening of the potential well when  $k_{\parallel}$  increases from zero, as noted in [4]. It is important that the correct determination of the moment when a new subband appears in a two-dimensional spectrum affects not only the quantitative assessment of

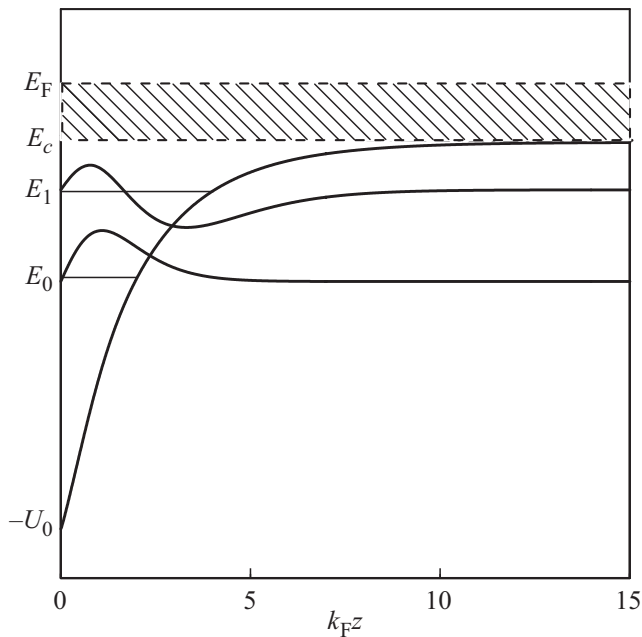


**Figure 1.** The potential well potential of the accumulation layer, the position of the minima of the two subbands and the corresponding wave functions normalized to unity are shown.  $E_c$  and  $E_F$  mark the position of the bottom of the conduction band and the Fermi level in the bulk,  $U_0$  — the band bending on the surface. Energies are referenced from the bottom of the conduction band in the bulk.

the density of quasi-two-dimensional electrons, but also allows for consideration of the intersubband scattering channel, even if the occupation of a new subband does not yet appear, for example, in the spectrum of magneto-oscillations.

The existing theoretical considerations of threshold dependencies in the literature are limited only to the threshold of the ground state entering the discrete spectrum, typically illustrated by a rectangular or sufficiently localized potential well. In the present work, the theory is generalized to the case of the appearance of excited states in order to also be able to determine accurately appearing of a new excited subband in the two-dimensional spectrum. This case is distinguished by the fact that the wave function of the  $n$ -th excited level has  $n$  nodes in the region of the well between the turning points and, accordingly, significantly deviates from zero in the intervals between the nodes (see Figure 1). In contrast, the unnormalized wave function of the shallow ground state, under the zero boundary condition at the well wall, remains small everywhere up to the turning point.

In addition, excited states appear in a potential well when its depth is significantly greater than the depth at which the ground state of a discrete spectrum emerges. Both of these factors increase the contribution of the integral over the region of the potential well to the normalization of the eigenfunction of the corresponding state relative to the contribution of the asymptotic neighborhood of

infinity, where the eigenfunction decreases exponentially. At the same time, the smallness of the contribution from the integral over the well region is usually considered the main condition for the applicability of the threshold approximation to the dependence of the spectrum on the depth of the potential well.

The second distinction of the potential of the accumulation layer from model rectangular or well-localized potentials is the slow, like  $1/z^2$ , decay of the self-consistent potential with imposed Friedel oscillations as one moves away from the surface (see numerical calculations in [5], Figs. 4 and 9). Such behavior at large distances is a universal consequence of the screening of the surface charge by a degenerate electron gas as follows from the results of the study [6]. Therefore, in the case of a potential obtained by solving a self-consistent system of Poisson and Schrödinger equations, it is required to determine what the boundary of the well is and where the asymptotic exponential decay of the solution begins. Both elements are essentially used in deriving the dependence of energy on the well depth near the threshold of the emergence of a new state in the discrete spectrum.

The noticeable deviation of the wave functions from zero in the well for excited states with low energy necessitated the consideration of the first correction to the threshold formulas, which takes into account the finite ratio of the contribution to the normalization integral from the well region to the contribution from the region of exponential decay. This allows expanding the scope of application of threshold formulas for determining the moment of appearance of a shallow state. Theoretical formulas were verified by numerical simulation of the energy spectrum of quasi-two-dimensional electrons in an accumulation layer on the surface of a degenerate  $n$ -InAs type semiconductor.

Currently, there are a number of works in which the assumption of the existence of a subband in the two-dimensional spectrum, starting at  $k_{\parallel} \neq 0$  is used to construct a physical picture of the observed experimental facts or to interpret the results of theoretical calculations in terms of „kinematic binding“ or a barrier formed by a coordinate-dependent effective mass (see [7–9] and references therein). Therefore, it seems important to establish the reality of the existence of such an unusual spectrum.

In this work, an attempt is made to answer posed questions through numerical modeling using semiconductor parameter values with a degenerate electron gas close to those studied experimentally. All calculations, the results of which are presented in the following sections, were carried out with the electron gas parameters for a typical direct-gap semiconductor, which was chosen as  $n$ -InAs with a donor concentration of  $N_+ \sim 1 \cdot 10^{17} \text{ cm}^{-3}$ . For the remaining parameters, the same values as in the work [4] were adopted: effective electron mass  $m^* = 0.023$ , bandgap  $E_g = 430 \text{ meV}$ , dielectric constant  $\epsilon = 12.6$ .

In the section „Parabolic conduction band“ the effective atomic units  $e^* = m^* = \hbar = 1$  are mainly used. The relationship between  $a.u.^*$  and usual atomic units  $a.u.$

is indicated in formulas (3.4) in [4]. In the section „Nonparabolic conduction band“ conventional atomic units are used.

In some cases, it is more convenient to normalize energy values to the Fermi energy of the ideal electron gas with the specified concentration, spatial coordinates — by multiplying by the Fermi quasimomentum. As a rule, this normalization is explicitly indicated.

## 2. Threshold effects in the spectrum of quasi-two-dimensional electrons with a parabolic conduction band in the bulk of a semiconductor

### 2.1. Problem statement

A  $n$ -type direct-bandgap semiconductor with a degenerate electron gas in the bulk is considered under conditions where an electron-attracting electric field is applied to the surface, generated either by the charge of positive ions adsorbed on the surface or by a voltage applied to a metal gate separated from the surface by a dielectric film. The band diagram of such a structure is presented in Figure 1. The energy spectrum of this problem is calculated using the method described in [4], as a result of solving the self-consistent system of equations for the wave functions  $\Psi_E$  and the electrostatic potential  $\phi$  (in dimensional units)

$$-\frac{\hbar^2}{2m^*} \Delta \Psi_E(\mathbf{r}) + U(\mathbf{r})\Psi_E(\mathbf{r}) = E\Psi_E(\mathbf{r}), \quad (1)$$

$$-\epsilon \nabla^2 \phi(\mathbf{r}) = 4\pi e(N_+ - N(\mathbf{r})), \quad (2)$$

$$N(\mathbf{r}) = 2 \int_{E \leq E_F} \mathfrak{D}\{E\} |\Psi_E(\mathbf{r})|^2, \quad (3)$$

under given boundary conditions on the eigenfunctions  $\Psi_E$  and the potential  $\phi$ . Here  $U(\mathbf{r}) = -e\phi(\mathbf{r})$  is the potential energy of the electron,  $E$  is the state energy,  $\mathfrak{D}$  denotes the differential spectral measure over the energy spectrum, and the integration is carried out over all occupied states, including size-quantized subbands.

### 2.2. Threshold effect formulas

Typically, the Schrödinger equation is considered, where the potential energy is proportional to the parameter  $\lambda$ . In the case of a rectangular well, its depth is directly proportional to this parameter. If at a certain threshold value  $\lambda_t$  the eigenvalue  $E = 0$  appears in the energy spectrum of the Schrödinger equation, then with a further increase in  $\lambda$  there is a shallow level in the well, whose binding energy depends quadratically on the detuning  $\lambda - \lambda_t$ . Such a dependence can be identified for many types of potential wells, for which explicit solutions of the corresponding Schrödinger equation exist. This suggests the existence of a threshold-type dependence in the case of a potential well of a sufficiently arbitrary form under certain conditions.

If the specification of the well potential is limited by the requirement that the Schrödinger equation has an eigenvalue  $E = 0$ , decays sufficiently rapidly to zero at infinity, and is proportional to the parameter  $\lambda$ , then the proof of the threshold behavior of the level depending on the detuning  $\lambda - \lambda_t$  is carried out in two ways in [10] (problem 4.27). Unfortunately, this conclusion is incorrect, and the correct result was obtained after unjustified assumptions. Therefore, we will follow the original idea of the threshold phenomenon, as it was formulated in the article by Bethe and Peierls [11]. This involves a weak dependence of the wave function of the shallow state on energy in the well region and the explicit form of the dependence of the wave function on energy far from the well in the region that provides the main contribution to the normalization coefficient. Similar considerations are also used in the theory of scattering of slow particles on a potential well with a shallow level (see [12] and Chapter IX in [3]).

The derivation of the threshold dependence of the binding energy without restricting the potential well's linear dependence on the parameter was presented in [13]. Here, only the formulas necessary as the basis for further transformations will be reproduced here.

Let the Schrödinger equation (in atomic units) with the potential  $U(z, \lambda)$  depending on the parameter  $\lambda$

$$\left[ -\frac{1}{2} \frac{d^2}{dz^2} + U(z, \lambda) \right] \Psi_{E(\lambda)}(z) = E(\lambda) \Psi_{E(\lambda)}(z) \quad (4)$$

have an eigenvalue  $E(\lambda_t) = 0$  at a certain value of the parameter  $\lambda_t$ . The problem is considered on the semi-axis  $0 \leq z < \infty$  with boundary conditions

$$\Psi_E(0) = 0, \quad \lim_{z \rightarrow \infty} \Psi_E(z) < \text{const.} \quad (5)$$

Regarding the potential, the asymptotic condition is considered to be satisfied

$$\lim_{z \rightarrow \infty} U(z, \lambda) \propto 1/z^{2+\alpha}, \quad \alpha > 0,$$

thanks to which two linearly independent solutions of equation (4) with  $E = 0$  have asymptotics at infinity of  $\sim \text{const}$  and  $\sim z$  according to Shpjets theorem [14]. If the solution  $\Psi_0$  remains bounded at infinity, then  $E = 0$  is eigenvalue and  $\Psi_0$  is eigenfunction.

To simplify the notation, let us introduce the designation of eigenfunctions as vectors in Hilbert space

$$\Psi_0(z) = |0\rangle, \quad \Psi_{E(\lambda)}(z) = |E\rangle. \quad (6)$$

Since the dependence of the energy  $E$  on the parameter  $\lambda$  near the threshold is being studied, we expand the potential as a function of  $\lambda$  into a series near the point  $\lambda_t$  up to first-order terms

$$U(x, \lambda) = U(z, \lambda_t) + \frac{dU(z, \lambda)}{d\lambda} (\lambda - \lambda_t). \quad (7)$$

Next, equation (4) at  $\lambda = \lambda_t$  is projected onto the state  $|E\rangle$ , and at the parameter  $\lambda$ , onto the state  $|0\rangle$ , and the first is

subtracted from the second. Considering the self-adjointness of the original equation, we derive

$$(\lambda - \lambda_t) \left\langle 0 \left| \frac{\partial U}{\partial \lambda} \right| E \right\rangle = E(\lambda) \langle 0|E \rangle. \quad (8)$$

Due to the locality condition of the potential energy  $U(z, \lambda)$  and the smallness of eigenvalue  $E(\lambda)$ , the main contribution to the scalar product  $\langle 0|E \rangle$  is given by the region outside the potential well, where the normalized eigenfunctions are known explicitly and are equal, respectively,

$$\Psi_0(z) = C_0, \quad \Psi_E(z) = C_E \exp(-\kappa z). \quad (9)$$

The normalization constants calculated with the same neglect of the well contribution are equal to  $C_0 = 1/\sqrt{2\pi}$  [15] and  $C_E = \sqrt{2\kappa}$ ,  $\kappa = \sqrt{2|E|}$ ,  $E = -\kappa^2/2$ .

Having calculated the scalar product on the right-hand side of (8) and explicitly restoring the matrix element expression on the left-hand side, we derive the formula

$$\frac{-\kappa^2}{2\kappa} = (\lambda - \lambda_t) \int_0^\infty dz \frac{\Psi_0(z)\Psi_E(z)}{C_0C_E(\kappa)} \left. \frac{\partial U}{\partial \lambda} \right|_{\lambda_t}, \quad \lambda > \lambda_t. \quad (10)$$

After obvious transformations, we derive an expression for the energy of a new level near the threshold of its appearance in the potential well

$$E(\lambda) = -2 \left[ \int_0^\infty dz \frac{\Psi_0(z)\Psi_E(z)}{C_0C_E(\kappa)} \left. \frac{\partial U}{\partial \lambda} \right|_{\lambda_t} \right]^2 (\lambda - \lambda_t)^2, \quad \lambda > \lambda_t. \quad (11)$$

This formula differs from the usually obtained quadratic dependence of the binding energy on the parameter near the threshold in that the energy clearly depends on the matrix element of the derivative of the potential with respect to the parameter  $\lambda$ . The normalization factor  $C_E(\kappa)$  depends significantly on energy. However, the solutions to the Schrödinger equations will not depend on the energy  $E$  in the well region after dividing by normalizing constants and are close to each other due to the identical initial condition  $\Psi_E(0) = 0$  and the smallness of the energy  $E$  relative to the potential energy  $U$  (see equation (4)).

Furthermore, under the integral, the difference between the eigenfunctions for the two energy eigenvalues is retained, which is usually neglected, reducing the integral to the average value of the potential over the eigenfunction for the zero eigenvalue. The latter is assumed to be constant and equal to one in the well region [16].

If the first approximation (before normalizing  $\Psi_{\lambda_t} \simeq \Psi_\lambda$  in the well region) is carried out with sufficient accuracy in all cases, the second will be incorrect when considering the appearance of the next  $n + 1$  bound state in the well, in addition to the already existing  $n$  state. This is because when  $E_{n+1} = 0$  and higher values of this parameter all solutions will have  $n + 1$  nodes in the well region in addition to the

zero boundary condition. As a result, the square of the wave function, even a shallow excited state, will take on large positive values in the region of the potential well, contributing significantly to the normalization integrals, as well as to the overlap integral  $\langle 0|E \rangle$  on the right-hand side of equation (8).

To extend the threshold approximation to the case of excited states, it is necessary to consider the consequences of rejecting the condition that the values of the normalization integral and the overlap integral are formed not in the region of the potential well but in the asymptotic region of exponential decay at infinity. Let us divide the overlap integral into two terms and estimate the contribution of each to the formula for the threshold dependence

$$\begin{aligned} \langle 0|E \rangle &= \int dz \Psi_0(z)\Psi_E(z) \\ &= C_0C_E \left[ \int_0^{z^*} dz \frac{\Psi_0(z)\Psi_E(z)}{C_0C_E} + \frac{1}{\kappa} e^{-\kappa z^*} \right] \\ &= C_0C_E \left[ I^{qw}(z^*) + \frac{1}{\kappa} + \frac{1}{\kappa} (e^{-\kappa z^*} - 1) \right]. \quad (12) \end{aligned}$$

Here,  $I^{qw}(z^*)$  denotes the contribution to the integral from the potential well region. The constants  $C_0, C_E$  account for differences between the eigenfunction  $\Psi_0(z^*)$  from unity and  $\Psi_E(z^*)$  from  $\exp(-\kappa z^*)$  (see (9)). Substituting (12) into equality (8), we obtain instead of (10)

$$\begin{aligned} \frac{-\kappa^2}{2} \left[ I^{qw}(z^*) + \frac{1}{\kappa} (e^{-\kappa z^*} - 1) \right] + \frac{-\kappa}{2} \\ = (\lambda - \lambda_t) \int_0^\infty dz \frac{\Psi_0(z)\Psi_E(z)}{C_0C_E} \left. \frac{\partial U}{\partial \lambda} \right|_{\lambda_t}, \quad \lambda > \lambda_t. \quad (13) \end{aligned}$$

The extinction constant  $\kappa$  is considered to be a small parameter of the theory. Therefore, the first term on the left-hand side is a quantity of the second order of smallness. The overlap integral cannot be greater than the normalization value, and even after dividing by the constants  $C_0, C_E$  and will remain on the order of unity. The largest number in square brackets can be the effective well size  $z^*$ , but it is multiplied by a small parameter — the binding energy. Thus, it follows from formula (13) under the condition  $\kappa^2 z^* < 1$ , there must exist a certain neighborhood of the parameter  $\lambda$  values near the threshold, in which the usual formula for the threshold dependence is preserved.

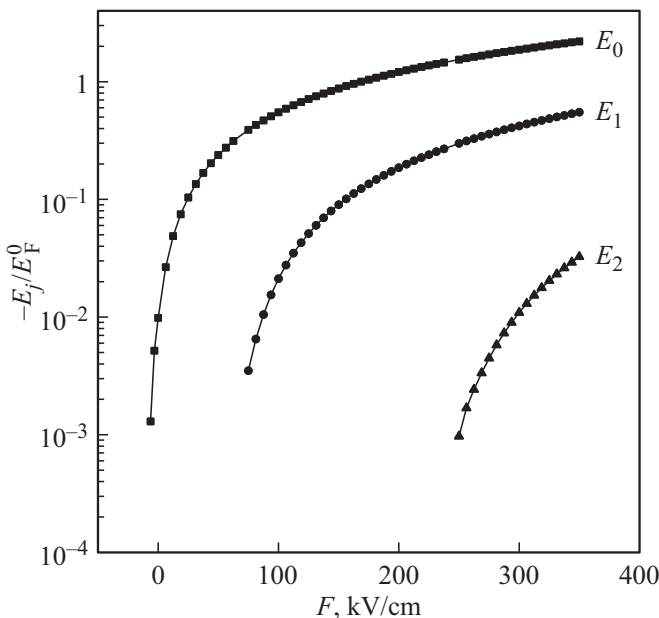
It should be noted that the equality (13) defines the parameter  $\lambda$  as a parabolic function of  $\kappa$  provided that the square bracket on the left side of (13) and the integral on the right side are weakly dependent on the energy  $E = -\kappa^2/2$ , and therefore on  $\lambda$ . Generally this allows determining the parameters of the parabola using the least-squares method and find the threshold value of the parameter  $\lambda_t$ . However, it is more convenient to do this in the area of linear

dependence between  $\kappa$  and  $\lambda$ , if such a region is sufficiently well defined. In any case, formula (13) enables the accurate determination of the threshold for the appearance of a new level. Moreover, the results of numerical simulation show that the region of linear dependence  $\lambda(\kappa)$  exists even in a self-consistent potential well and is quite sufficient for determining threshold values.

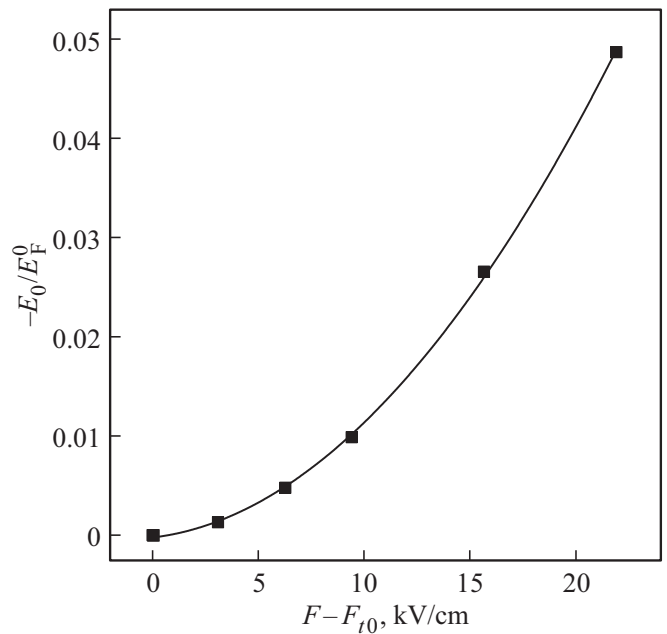
### 2.3. Results of the numerical experiment

Figure 2 shows the results of self-consistent calculations of the dependence of the energy spectrum of quasi-two-dimensional electrons in the accumulation layer on the electric field  $F$  applied to the surface. New size-quantized subbands are observed to appear with the increase of the electric field strength. In a small neighborhood of field values where a new subband appears, the iterative solution of the self-consistent Poisson–Schrödinger equation system ceases to converge, leading to gaps in the curves.

The mechanism of this loss of convergence when a shallow bound state appears is discussed in [5] (end of section 3.2) and in [4] (Appendix A). Here we demonstrate that the threshold theory allows us to determine the field values at which a new subband appears in the two-dimensional spectrum. Although exactly at such values, a self-consistent calculation of the electronic spectrum is impossible.



**Figure 2.** The position of the subbands minima in the energy spectrum of quasi-two-dimensional electrons in the accumulation layer of an  $n$ -type semiconductor as a function of the electric field applied to the surface. To induce the appearance of the shallow main subband,  $E_0$ , a negative field had to be applied to the surface to reduce the depth of the Konstantinov-Shik self-consistent potential well until the dimensional quantization level disappeared (see the discussion of this phenomenon in Ref. [5], section 3.1).



**Figure 3.** Determination of the threshold field  $F_0$  for the appearance of the main subband by fitting the parameters of the parabolic dependence according to formula (11) using the least-squares method for four calculated points (black squares for  $F - F_{t0} > 0$ ). The threshold field was determined by selecting the position of the fifth point, taking into account the requirement that the minimum of the parabola lies on the abscissa axis.  $F_{t0} = -10.4$  kV/cm.

Figure 3 shows the result of fitting the threshold field value for the main subband  $E_0$  shown in Figure 2. The four points at the final detuning values  $F - F_c$  are taken from the calculated curve  $E_0$ . The  $F_c$  field, which determines the position of the fifth point, was selected so that drawing a parabola through the five points using the least-squares method would result in a curve tangent to the  $x$ -axis. It was possible to do this with a certain accuracy, but in the absence of software implementation, the process turned out to be quite tedious.

However, formula (10) and, especially, (13) suggest that it would be more convenient to use the region of the linear dependence of the extinction constant  $\kappa$  on the parameter, in this case the field  $F$ , on the plane  $(\kappa, F)$ . Then extrapolating the right line to the point where  $\kappa = 0$  will allow us to determine the threshold field  $F_{t0}$  for the main subband. The implementation of such a construction is presented in Figure 4, where the exponent decay constant is replaced by the normalized value  $|k_z|/k_F$ .

Table 1 summarizes the results of this extrapolation. The third column of the table shows the minimum field values, starting from which a self-consistent iterative calculation allows to find the minimum energy for a given subband. Figure 4 shows that the linear dependence is replaced by a nonlinear one at an extinction parameter of the order of 0.3. According to Formula (13), this allows

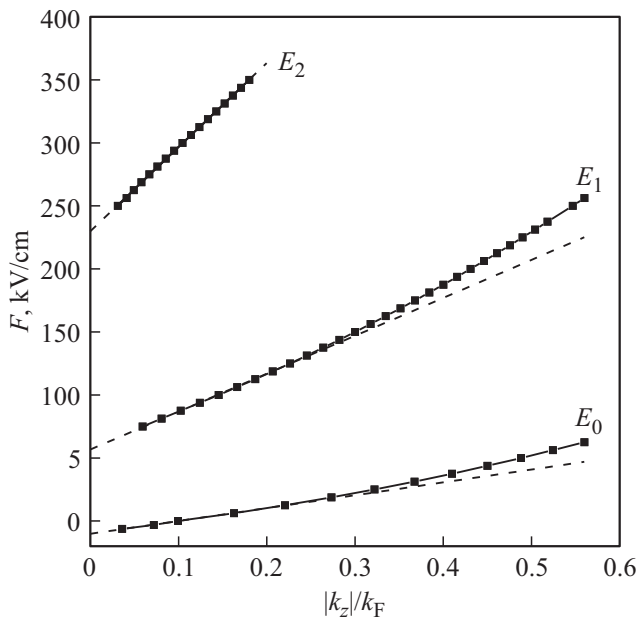


**Figure 4.** The initial sections of the curves presented in Figure 2 are reconstructed in the corresponding coordinates.

us to estimate coefficient for the square of the extinction constant.

In any case, under the parameters of the conducted calculation, which are, as shown in [4], close to the characteristics of real objects, the region of a purely threshold linear dependence is clearly noticeable and can be used to refine the threshold field values.

With the threshold field values known accurately, we can consider the position of the subband minima on a much larger scale of field changes. The result of this approach is presented in Figure 5. It is evident that the characteristic quadratic dependence of the binding energy on the parameter, which modifies the depth of the potential well, spans approximately one and a half orders of magnitude and can be effectively used to refine the threshold field based on experimental data.

In conclusion of this section, Figure 6 shows the result of testing the applicability of the threshold theory to the energy level localized in a self-organizing Konstantinov–Shik potential well. The details of the spectrum calculation are described in the paper [5]. The dependence of the depth of the effective potential well of the density functional theory

**Table 1.** The threshold fields for three subbands of Figure 2, determined from Figure 4

Number subbands	Equation of the right line Figure 4	Threshold field $F_t$ , kV/cm	Minimum field, kV/cm
$E_0$	$E_0 = 105.3 k_z  - 10.4$	-10	-6.5
$E_1$	$E_1 = 300.9 k_z  + 56.7$	57	75
$E_2$	$E_2 = 667.9 k_z  + 229.8$	230	250

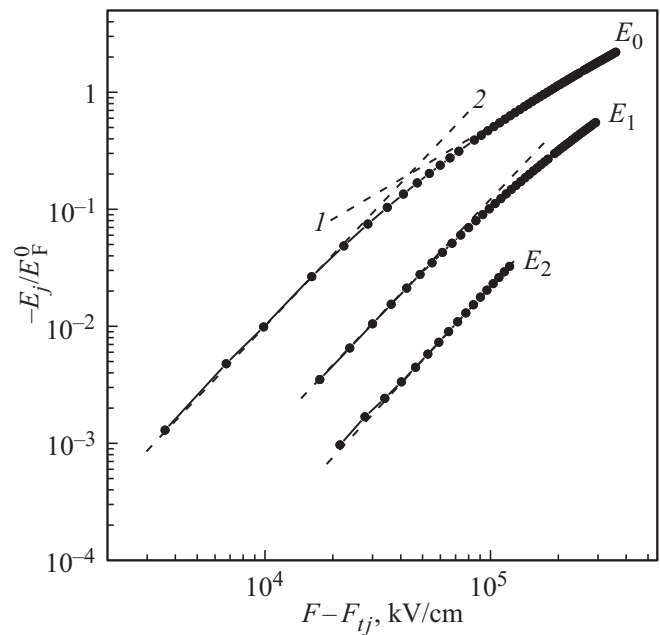


**Figure 5.** The minimum energies of the three calculated subbands of size quantization, presented in Figure 2, plotted as a function of the excess over the threshold field value for each subband. The dashed lines show the slopes of the power-law dependence of the minimum energy on the detuning. The number 2 marks the parabolic slope corresponding to the threshold formula (11). The number 1 indicates a commonly observed linear dependence. The threshold fields are provided in Table 1.

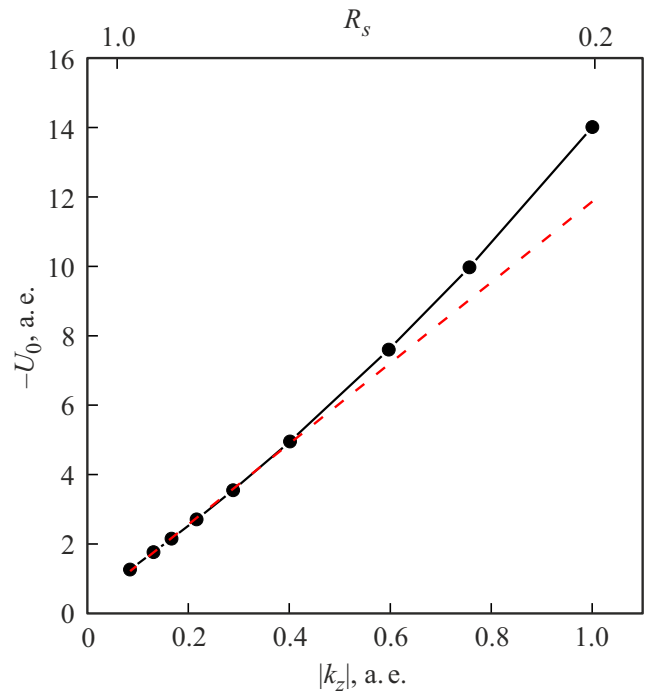


**Figure 6.** Dependence of the potential minimum  $U_0$  potential in the self-organizing potential well near the impenetrable boundary of a degenerate electron gas on the extinction constant of the wave function in the bulk. The level energy  $E = -|k_z|^2/2$ .

on the extinction parameter of wave functions in the volume is plotted using curves numbered 1 in Figure 4, *a, b* of the article [5]. The dependence of the level energy on  $R_s$ , curve 1(b), was refined in [4], Figure 11.

The presence of a rectilinear section in Figure 6 clearly demonstrates the validity of the threshold approximation in a certain vicinity of the moment of appearance of the bound state and in the case of a nonlinear dependence of the Poisson solution on the parameter — positive background density.

The approximation of the calculated dependence by a straight line, in principle, allows answering the question posed in the paper [17] about the boundary of the existence of such a bound state. For this purpose it is necessary to find the value  $U_0$  from Figure 6 and the corresponding value  $R_s$ , at which  $|k_z| = 0$ .

### 3. Nonparabolic energy spectrum of the semiconductor conduction band

The case of the energy spectrum of quasi-two-dimensional electrons of an accumulation layer on the surface of a direct-bandgap semiconductor is considered, taking into account the finite width  $E_g$  of the bandgap within the framework of the two-band Kane model. Spectra are calculated using the effective mass equation for the nonparabolic conduction band [18], the solution method of which is described in [4]. The dispersion law  $E_j(k_{\parallel}, k_z)$ , unlike the parabolic case, non-trivially depends on the components  $k_{\parallel}$  of the quasimomentum along the surface of the semiconductor due to the dependence of the binding energy  $k_z^2$  on  $k_{\parallel}$  (see [4], Figure 7, *b*).

The electrostatic potential energy  $U(z)$  of electrons enters the effective mass equation at  $E_g \neq 0$  through the energy-dependent quasipotential  $U_{qp}(U, E)$ . As a consequence, threshold effects in this case are determined not by one parameter such as the gate voltage  $V_g$ , but by two:  $V_g$  and  $k_{\parallel}^2$ . The dependence  $E_j(V_g)$  at  $k_{\parallel} = 0$  will be analogous to the dependence in Figure 2 with a similar inability to obtain a self-consistent solution in the vicinity of the creation of a new subband.

However, a peculiar threshold behavior will be present in  $E_j(k_{\parallel})$ -dependence for a fixed value of  $V_g$  and therefore  $U(z)$ . The main feature of this case is that the minimum detectable value of the bottom position of the  $j$  subband  $E_{jm} = E_j(0)$  at given  $V_g$  not zero, but is equal to a small but finite negative value. The threshold behavior in this case occurs in the dependence  $E_g(k_{\parallel})$  in the vicinity of the bottom.

At small negative energy values  $E$ , the corresponding wave functions  $\Psi_E$  have a large spatial extent beyond the boundary of the potential well deep into the semiconductor. This results in instability in the iterative solution process of the self-consistent system of effective mass and Poisson equations. However, the same large spatial extension of wave functions from this region of low binding energies

makes it possible to analyze the energy spectrum using the threshold effect theory.

#### 3.1. Refinement of the threshold theory in the case of a quasipotential in the effective mass equation for a nonparabolic conduction band

Let the minimum  $E_m(0, k_{zm}^2)$  of the size-quantized subband lie close to the boundary of the continuous spectrum of a given quasipotential well  $U_{qp}(z)$ . We will find the dependence of the energy on the quasimomentum  $k_{\parallel}$  parallel to the surface. To do this, we consider the effective mass equation for the nonparabolic conduction band in the two-band approximation (see [4], equations (4.17), (4.39)) at two energy values  $E$  and the condition  $k_{zm}^2 < 0$ .

$$\left[ -\frac{\hbar^2}{2m_c^*} \frac{d^2}{dz^2} + U_{qp}(z, E_m) \right] \Psi_{E_m}(z) = k_{zm}^2 \Psi_{E_m}(z), \quad (14)$$

$$\left[ -\frac{\hbar^2}{2m_c^*} \frac{d^2}{dz^2} + U_{qp}(z, E) \right] \Psi_E(z) = k_z^2 \Psi_E(z). \quad (15)$$

Here, the quasipotential is defined by the formula

$$U_{qp}(z, E) = U(z) \left( 1 + 2 \frac{E}{E_g} \right) - \frac{U^2(z)}{E_g}. \quad (16)$$

The dependence of the energy  $E(k_{\parallel}, k_z)$  on quantum numbers is given by the roots of the dispersion equation

$$2m_c^* E \left( 1 + \frac{E}{E_g} \right) = k_{\parallel}^2 + k_z^2, \quad (17)$$

corresponding to the conduction band

$$E_c = \frac{E_g}{2} \left( \sqrt{1 + \frac{2(k_{\parallel}^2 + k_z^2)}{m_c^* E_g}} - 1 \right) \quad (18)$$

and the valence band

$$E_v = -\frac{E_g}{2} \left( \sqrt{1 + \frac{2(k_{\parallel}^2 + k_z^2)}{m_c^* E_g}} + 1 \right), \quad (19)$$

where  $E_g$  is a bandgap width.

By assumption, the asymptotic behavior of the eigenfunctions at infinity is determined by the condition  $\lim_{z \rightarrow \infty} U(z) = 0$  imposed on the electrostatic potential. Accordingly, in this area we have

$$\Psi_{E_m} = C_m \exp(-|k_{zm}|z), \quad \Psi_E(z) = C_E \exp(-|k_z|z). \quad (20)$$

Note that the quasipotential in formula (16) depends explicitly on the energy of the two-dimensional state, which is why the difference in the projections of equations (14) and (15) onto the corresponding eigenvectors will contain the energy difference  $E - E_m$  at a constant electrostatic potential. When calculating the non-parabolic two-dimensional subband as a function of  $k_{\parallel}^2$ , the energy changes with the

change in lateral quasimomentum at a constant external field. Thus, after evaluating the overlap integral  $\langle E_m | E \rangle$  using the explicit expressions for the eigenfunctions (20), we obtain a threshold theory relation where the parameter affecting the depth of the potential well is the total energy of the two-dimensional state. The role of the binding energy is played by the square of the quasimomentum component normal to the surface. As a result, we obtain a relation of the form of the threshold formula between the total energy  $E$  and the localization energy of the degree of freedom normal to the surface

$$E - E_m = \frac{E_g}{2\tilde{I}} [|k_z| - |k_{zm}| + (|k_z|^2 - |k_{zm}|^2)] \times (I^{qw}(z^*) - z^*). \quad (21)$$

Here, all variables are normalized to  $E_F^0$  and  $k_F$ , respectively. The integral  $\tilde{I}$  is the matrix element of electrostatic potential energy

$$\tilde{I} = \left[ \int_0^\infty \frac{\Psi_E(z)}{C_E(k_z)} U(z) \frac{\Psi_{E_m}(z)}{C_{E_m}(k_{zm})} dz \right], \quad (22)$$

$I^{qw}$  denotes the incomplete overlap integral

$$I^{qw}(z^*) = \left| \int_0^{z^*} dz \frac{\Psi_E(z)\Psi_{E_m}(z)}{C_E(k_z)C_{E_m}(k_{zm})} \right|. \quad (23)$$

In general, equation (21) is structurally similar to (13). The primary distinction is the appearance of the difference between the energy at the minimum and the energy of the state at finite  $k_{\parallel}$ . Therefore, even in the case of a quasipotential, one can expect the existence of an energy region where the threshold theory conditions for the spectrum  $E_j(k_{\parallel})$  are satisfied.

### 3.2. Results of numerical experiments

Figure 7 shows the calculated self-consistent two-dimensional spectrum of electrons in the potential well of the accumulation layer near the surface. An electron-attracting potential, creating a band bending of  $-435$  meV, is applied to the surface. It was not possible to calculate the low binding energy of the minimum of the second excited subband in this calculation. The convergence issue of the iterative procedure for the self-consistent solution and the irregular method used to circumvent them are described in [4]. Here we attempted to develop a regular method to eliminate the known difficulties in numerical calculation of very low binding energies, which are caused by the large spatial extent of the eigenfunctions of such states and the limited interval over which real calculations can be carried out.

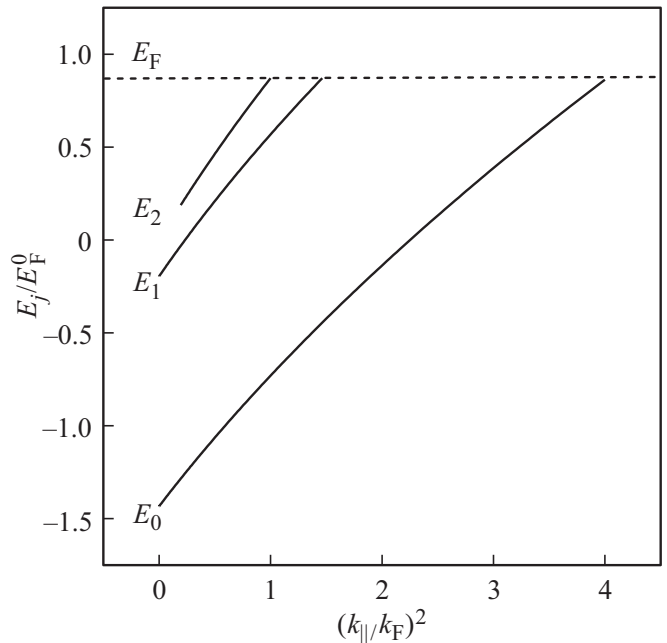


**Figure 7.** The energy spectrum of quasi-two-dimensional electrons of the accumulation layer on the surface of a degenerate  $n$ -type semiconductor. The position of the Fermi level below unity reflects the nonparabolicity of the spectrum in the bulk. It should be noted that the calculation failed to obtain the spectrum of the second excited subband  $E_2$ , which would begin at  $k_{\parallel} = 0$ .

#### 3.2.1. Standard calculation algorithm

To begin with, calculations of the spectrum were carried out at three values of the surface potential, when either the main subband  $E_0$ , or the first excited subband  $E_1$ , or the second  $E_2$  turns out to be shallow. All three spectra in the coordinates of threshold variables are shown in Figure 8. The two graphs  $E_0(|k_z|)$  and  $E_1(|k_z|)$  change in a regular way with the deepening of the quasipotential well and both show the intersection of the abscissa axis at  $|k_z| > 0$ . This corresponds to the existence of a negative energy of the subband minimum at  $k_{\parallel} = 0$ , since in this case with great accuracy  $E_m(0, k_z) = -|k_{zm}|^2$  (normalization to  $E_F^0$  and  $k_F$ ).

It should be noted that in reality, finding  $|k_{zm}|$  from equation (21) in the case of a normal form of the dependence  $E_j(|k_z|)$  is somewhat more complex than determining the moment of appearance of a new subband in the case of a parabolic zone from the intersection of the straight line with the ordinate axis in Figure 4. First, one must set  $E_m = -|k_{zm}|^2$ , then it is necessary to find the coefficients for all powers of the quadratic trinomial with respect to  $|k_{zm}|$  by approximating the calculated set of pairs  $(E_j, |k_z|)$  with a parabola. The found coefficients should be used to solve the quadratic equation obtained from (21) with respect to  $|k_{zm}|$ , assuming, for example,  $E = 0$  and finding the corresponding value  $|k_z|$ . After that, set  $E_m = -|k_{zm}|^2$  (normalization to  $E_F^0$  and  $k_F$ ). The procedure can be



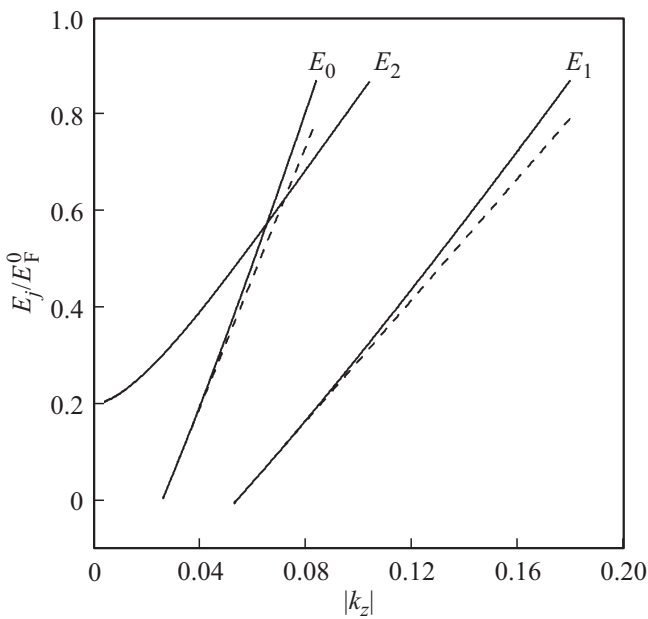


**Figure 8.** Inverted dependence of the localization energy  $\sqrt{-k_z^2}$  on the quasipotential parameter — energy  $E$  of the two-dimensional state. A sharp difference is observed between the graph of the second excited subband  $E_2$  and the graphs for the main and first excited subband. All three graphs were calculated at different values of the surface potential, selected so that the corresponding level was at the detection limit in our calculations. It should be noted that the higher the serial number of the subband in this figure, the deeper the corresponding well of the electrostatic potential. The electrostatic potential remains constant along all curves. The quasipotential changes in connection with changes in energy  $E$ .

simplified if there is a sufficiently long linear section with respect to  $|k_z|$ . However, relative to the minimum value  $|k_{zm}|$ , the quadratic equation will still be necessary to solve.

**3.2.2. The study of the anomalous threshold dependence of the second excited subband  $E_2$**

To determine the reasons behind the emergence of a non-physical energy dependence on the quasimomentum, as seen in the  $E_2$  graph, possible mathematical roots for the inaccurate determination of the near-zero eigenvalue of the effective mass equation were examined. The impact of transferring the zero boundary condition on the solution from infinity to the end point  $L$ , the boundary of the computational interval, was evaluated. This gives rise to an admixture of growing exponential in the solution in the vicinity of the point  $L$ , but with the selected values  $L$  gave differences only in the third or fourth decimal place and was discarded.

The second possible reason is the non-standard form of the quasipotential, which consists of two terms and only one of them changes with the variation of the parameter  $E$ . To test this, a similar calculation was performed for three cases

of shallow subbands — the main, first and second excited — in a rectangular potential well. The quasipotential (16) of such a well remains a rectangular well, but now consists of two terms.

The calculation results are presented in Figure 9. It is evident that in this case all three shallow subbands change with the depth of the potential well in a systematic manner. The corresponding minimum values for the potentials at which each subband appears are indicated in the caption to the figure. These results showed that the threshold theory is quite valid for the first two subbands. The reason for the anomalous behavior of the third subband remains unclear. It could be assumed, however, that the number of nodes in the region of the quasipotential well between the turning points is not such a reason, as the eigenfunctions of the second excited subband are the same in both the quasipotential well of the electrostatic potential and the rectangular one.

There was one more place in the calculation program that could give rise to unclear consequences. Since the iterative solution did not converge to the required accuracy without considering the contribution to the electron density from the full spectrum of the subband  $E_2$  in Figure 7, a forced wave function, identical for all  $k_{||}$  values, was applied during the calculation of this contribution for the spectrum range  $0 \leq k < k_c$ , based on the assumption that in this range of low binding energies, all functions differ little in the region of the potential well.

After eliminating this procedure, the iterative solution, indeed, ceased to converge in the sense that the usual criterion for exiting the self-consistency loop at the level of the difference between the input and output of the order  $1 \cdot 10^{-5}$  was not achieved. But there was no unlimited

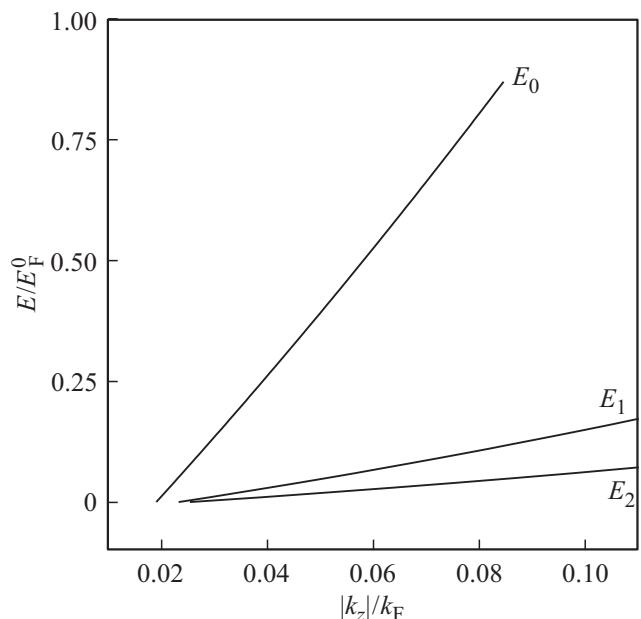


**Figure 9.** Dependence  $E_j(|k_z|)$  for shallow subbands in the case of a rectangular quasipotential well. The width of the seed potential well is 5.0, with depths  $U_0 = -0.105$  ( $E_0$ ),  $-0.795$  ( $E_1$ ),  $-1.89$  ( $E_2$ ). There is no anomalous behavior.

growth in the self-consistency error. Moreover, it turned out that in this mode two types of possible solutions, presented in Figure 10, began to alternate regularly. One is completely non-physical, type  $E_2$  in Figure 8. The other shows a more reasonable, at first glance, behavior in the sense of a natural intersection of the  $x$ -axis at  $|k_z| > 0$ . This behavior persists even when extending the calculations to about 40 cycles. That is, a stable state of the used algorithm for a self-consistent solution of a system of nonlinear equations has appeared.

To verify whether the dependences of the type of the 18th or 20th cycle located in the correct parameter range are normal, Figure 11 jointly presents the dependences  $E_0$  and  $E_1$  from Figure 8 and the dependence  $E_2^{(18)}$  from Figure 10. The figure shows that these dependencies do not belong to the same family.

It remained to determine if the strange behavior of the third subband spectrum was caused by the slow decay of the self-consistent electrostatic potential. In principle, from the theory of surface charge screening it is known that at large distances from the surface the potential decreases as  $1/z^2$ . Such a slow decrease is borderline for the opportunity of considering the neighborhood of infinity as a region where the solution for  $U(z) \equiv 0$  can be used as an asymptotics. However, the presence of potential modulation by Friedel oscillations left the opportunity that these oscillations produces a faster effective decay of the potential to zero.

This question can be addressed by evaluating the correction to the basic threshold formula, which is described by the terms in parentheses of the formula (21). To do this, it is necessary to know where the region of exponential behavior of the numerically found solutions begins and how well it is expressed. A good indicator of the region of exponential dependence of a solution can be the logarithmic derivative of the solution, which in this region tends to a constant equal to the decay (or growth) constant.

From this point of view, the relationship between the logarithmic derivative and the phase  $\phi(z)$  proved to be convenient, which is found using the trigonometric sweep method we employ in the form  $\psi'(z)/\psi(z) = \text{tg}(\phi(z))$  proved to be convenient. In Figure 12, the graphs of the wave function, phase tangent and normalization integral as a function of the upper limit are plotted for the state  $E = 0$  of the shallow subband  $E_1$ . The boundary of the quasipotential well is taken as the point  $z^*$ , where the tangent becomes equal to the known value of the extinction constant  $-|k_z|$  with an accuracy of three decimal places.

It can be seen that simultaneously, at the point  $z^*$ , the normalization integral almost reached its limit value of one. As expected, the wave function of the first excited state has one zero inside the well between the turning points for the given binding energy  $-|k_z|^2$ .

For the convenience of comparing curves calculated with different parameters, their characteristics were summarized in Table 2. The data were taken from the calculated wave

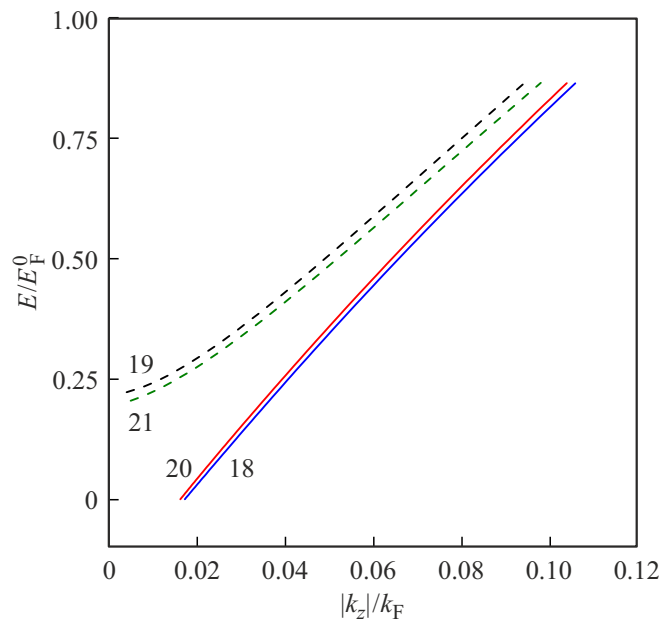


**Figure 10.** Two types of solution of a self-consistent iterative algorithm in the case of a shallow second excited subband  $E_2$ . The surface potential, measured from the Fermi level, is equal to  $-445$  meV. The numbers near the curves indicate the numbers of cycles of the self-consistent procedure for sequentially solving the system Poisson equation — effective mass equation for a nonparabolic conduction band. It can be seen that the differences between curves of the same type are small, less than between curves of different types. However, there is no convergence with a given accuracy even within one type; there are fluctuations in the order of the differences between the curves in the figure.

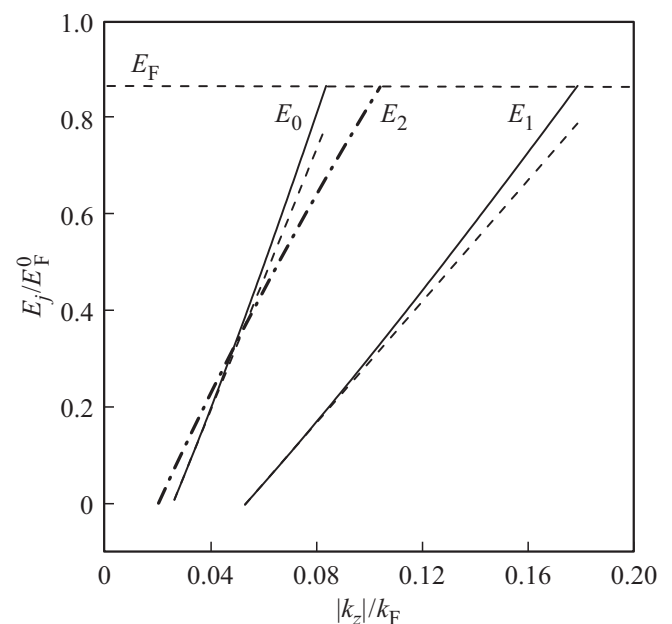


**Figure 11.** Three threshold dependences for shallow subbands of the ground, first and second excited states, taken from Figure 8 ( $E_0$  and  $E_1$ ) and Figure 10 ( $E_2^{(18)}$ ). There is no similarity between the behavior of the first two dependences and the third when the quasipotential well is deepened.

**Table 2.** Table of parameters and results  $E_F^0 = 71.46$  meV

Number subbands	Parameters			Results			
	$F_s$ kV/cm	$U_s$ meV	$E/E_F$	$ k_z /k_F$	Turning point $z_t$	$z^*$	$I^{qw}(z^*)$
$E_0$	-5	-18.6	0.00	0.026	13.44	62.0	0.925
			0.18	0.039	11.72	60.9	0.992
$E_1$	136	-160.0	0.00	0.053	12.08	51.7	0.994
			0.25	0.093	10.51	49.5	0.999
$E_2^{(18)}$	471	-382.6	$-2.7 \cdot 10^{-4}$	0.017	25.97	61.54	0.812
			0.25	0.042	20.36	61.2	0.987

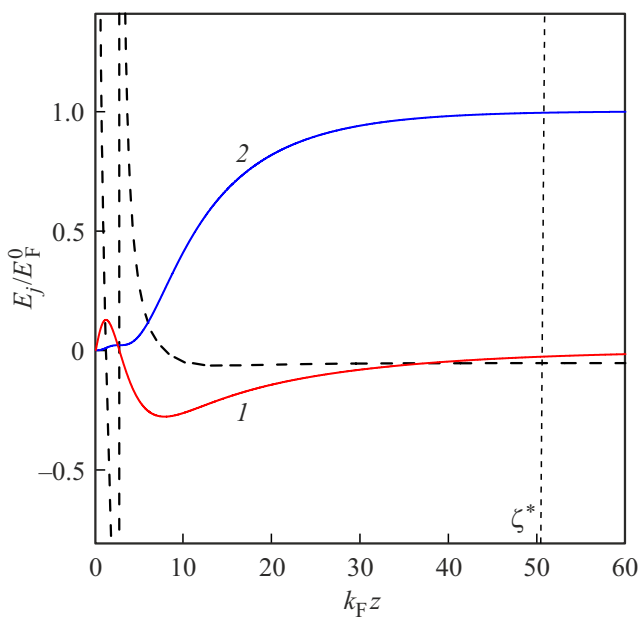


**Figure 12.** Curve 1 represents the wave function of the state for  $E = 0$  of the first excited subband  $E_1$ . Curve 2 shows the dependence of the integral of the square of this wave function as a function of the upper limit. The dashed curve represents the spatial dependence of the phase tangent on the coordinate  $z$ . The vertical dashed line marks the position of the  $z^*$  point. The potential well is created by the field of 136 kV/cm.

functions for two characteristic points on the graphs of all subbands: at  $E = 0$ , i.e. near the bottom of the subband, and at the upper boundary of the linear section, which was used to refine the energy at the minimum of the subband. Although this latter procedure did not improve the results obtained with the larger length  $L = 350$  of the computational interval and, consequently, significantly increased computation time.

Analysis of the table showed that the  $E_2$  data indicate, first of all, an increase in the width of the potential well as its depth increases due to an increase in the field on the surface. In contrast, when moving from the field where the main subband  $E_0$  is shallow to a higher field where the first

excited subband  $E_1$  becomes shallow, the well narrowed due to an increase in the surface charge density of the quasi-two-dimensional electrons as the wells depth increased.

Conversely, as the well widened with increasing field, the calculation yielded an insufficient excess electron density in the states of the two-dimensional spectrum near the surface. This lack of electrons is compensated by the mechanism embedded in the algorithm that changes the distribution of electrons in the bulk, which ensures that the electric field vanishes at infinity and in this case results in a smooth broadening of the potential well.

It is important to emphasize that in the case of  $n$ -InAs under consideration, to appear in the spectrum of the second excited subband, a field must be applied to the surface, where the band bending at the surface almost matches the width of the bandgap. This allows us to suggest that the answer to the question of where the missing electrons in surface states might be located should be sought in the possible formation of two-dimensional valence surface subbands.

With such a strong band bending by the external field that the minimum of the quasipotential may be below the top of the valence band, the effective mass equation (17) in the two-band Kane model may have solutions with energy  $E$  in the bandgap below its middle  $-E_g < E < -E_g/2$ . These states should be sought in the form of an expansion in terms of the basis of the Bloch functions of the valence band with the dispersion law in the form of the second root  $E_v(k^2)$  (19) of the dispersion equation. Since the initial energy of these states is in the bandgap over the top of the valence band, in an undoped semiconductor they are not occupied by valence electrons. But in the case of doping of the conduction band, electrons from there can transit to the free states of the two-dimensional valence band and form the missing surface charge.

Thus, the mechanism for the appearance of two types of  $E_2(|k_z|)$  dependence can be represented as follows. Since the calculation did not take into account the opportunity of the formation of two-dimensional valence subbands occupied with electrons, when solving the nonlinear Poisson equation (2) (with clarification for the nonparabolic band spectrum see section 4.1.3 in [4]) the deficit in density of

quasi-two-dimensional electrons was compensated by the formation of a self-consistent wide potential well, the shape of which differs from the regular shape of the well formed by a sequential increase in the surface field.

In the widened well, in the next self-consistent cycle, a shallow subband from the conduction band states is determined, which is occupied with electrons. As a consequence, the well narrows, and the states of the second excited subband at  $k_{\parallel} = 0$  and in the immediate vicinity become so shallow that they do not appear until the deepening of the quasipotential well due to the growth of  $E \approx k_{\parallel}^2$  makes the energy level  $k_z^2(k_{\parallel}^2)$  exceed the detection threshold ( $\simeq -1.5 \cdot 10^{-4} E_F^0$  in our case). This leads to a two-dimensional spectrum with the subband  $E_2$  of the type shown in Figure 7. Accordingly, when integrating over the spectrum, there is no contribution the  $E_2$  states in the  $0 < k_{\parallel} < k_{\parallel c}$  region and again there is a lack of electron charge density in two-dimensional states. This again causes a broadening of the self-consistent well, where the entire spectrum of the second excited subband can be calculated, but the quasipotential well takes on a different shape.

### 3.3. Finding

Given the multifaceted nature of the results obtained in this section, it makes sense to discuss their implications separately.

#### 3.3.1. On the hypothesis of the existence of two-dimensional spectra starting from $k_{\parallel c} \neq 0$

The assumption made in the article [2] about the possible existence of the subband  $E_j(k_{\parallel})$  in the two-dimensional spectrum of a semiconductor with a non-parabolic conduction band accumulation, that starts from a non-zero value of the lateral quasimomentum  $k_{\parallel c} \neq 0$ , is based on two facts.

The first is the peculiar behavior of the spectral curves (figure 2 in [2]), calculated with the consideration of the screening of the external field not only by electrons in two-dimensional states, but also by bulk electrons. The second is a characteristic pattern of the dependence of the number of electrons in the first excited subband on the gate voltage  $V_g$  at the initial stage of its appearance (see inset on Figure 3 in [2]). This dependence was measured in the paper [19] and clearly corresponds to the threshold dependence presented here in Figure 3. Consequently, the fact of experimental evidence in favor of the discussed assumption can be excluded from consideration.

As for the model spectrum of the excited subband in Figure 2 in [2], then it qualitatively resembles the graph of the subband  $E_2$  in Figure 7 since it also begins at  $k_{\parallel c} \neq 0$  and the initial energy falls into the region of the continuous spectrum. However, regarding our calculation, analysis of the characteristics of the  $E_2$  graph according to the data presented in Table 2 shows that this was a bound state in a completely different quasipotential well. This well is much wider, if we compare the position of its turning

points with the positions of the turning points for the usual subbands  $E_0$  and  $E_1$ , and it decays more slowly to zero at infinity. The possible reasons for the appearance of such a wide potential well in the case of a shortage of quasi-two-dimensional electrons to screen the external field are explained in Section 3.2.2. In turn, a very shallow level may appear in a wide potential well, the binding energy of which is beyond the resolution of a specific implementation of the algorithm, as explained in [4] (Appendix A.1).

Thus, there is no experimental confirmation of the existence of size-quantized subbands  $E_j(k_{\parallel})$  with  $k_{\parallel min} \neq 0$ . As for the opportunity of this type of spectrum appearing in calculations for a nonparabolic conduction band, in our case, firstly, it appears under bandbending comparable to  $E_g$ , where the question must be raised about the possible influence of two-dimensional subbands corresponding to the valence band on the result.

Secondly, it should be borne in mind that at very low binding energies and energies  $E$  near the boundary of the continuous spectrum, the energy of the size-quantized level  $k_z^2$  turns out to be a very slowly varying function  $k_{\parallel}$ . Namely, if we put  $E_m = k_{zm} = 0$  in equation (21) and take into account that near the boundary with a continuous spectrum and low binding energy  $E \simeq k_{\parallel}^2$ , then we obtain  $k_z^2 \sim k_{\parallel}^4$ . This fact means that as  $k_{\parallel}$  increases, the energy level will slowly exit the undetectable region. At the same time, the total energy of the level will increase, since  $E = k_{\parallel}^2$ , and will reach values in the region of the continuous spectrum by the time the final value of the binding energy appears in the calculation. This is what is seen in Figure 7.

The results of calculations of the two-dimensional spectrum of electrons in the accumulation layer on the  $n$ -InAs. surface, presented in the work [20], cannot also be considered as proof. For such a subtle issue, they were obtained with a too short length of the calculated interval ( $k_{Fz_{max}} = 16$ ), using an approximate iterative method (mixing scheme [21]) during a self-consistency process, which may provide a small difference between the input and output of the iterative scheme, but does not provide any information about the degree of proximity to the real solution (see the discussion in [22]).

#### 3.3.2. The role of valence band states in the two-dimensional spectrum of the accumulation layer

It was noted in Keldysh's work [23] on deep levels in semiconductors that the presence of the  $-U^2/E_g$  term in the effective mass equation (15) implies that this potential attracts carriers of any sign. This fact was pointed out as a possible explanation for the formation of discrete spectrum states by some impurities deep within the bandgap both for electrons and holes. Such an explanation of the known amphoteric behavior of impurities with deep levels was linked precisely to their location near the middle of the bandgap. Therefore, it is desirable to understand, so far at least in principle, whether the formation of two-dimensional

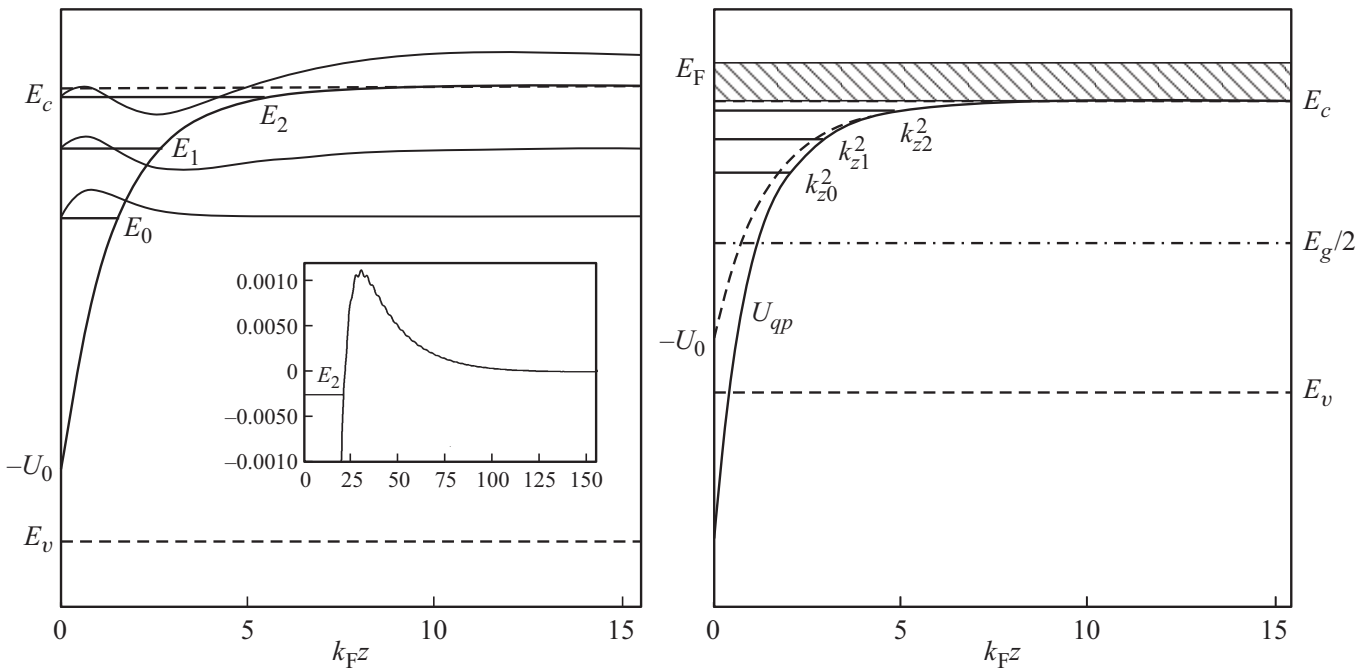


**Figure 13.** Left panel. Energy diagram of the accumulation layer for the case of the surface potential, when the second excited subband  $E_2$  appears. The graph of the potential energy, the positions of the minima of the subbands ( $E_2$  is shown schematically due to the proximity to zero of the energy scale, see Table 2), and the wave functions of the corresponding states are shown. The inset represents the position of the minimum energy of the  $E_2$  subband relative to the potential energy graphics near the turning point  $z_{ij}$ . Note the absence of noticeable Friedel oscillations at this scale. Right panel. The position of the quasipotential for the bottom energy of the subband  $E_2$  generated by the potential in the left figure, relative to the edges of the bandgap. The positions of the minima of each subband are marked ( $k_{z2}^2$  again is shown schematically). The dashed curve is potential energy from the left panel. The shaded area above the bottom of the conduction band indicates occupied states of the continuous spectrum.

valence subbands in a deep potential well for electrons is possible.

The graphs of the potential  $U$  and the quasipotential  $U_{qp}$  in Figure 13 show that formally the Schrödinger equation with such a potential (in fact — the effective mass equation (15) with such a quasipotential) could have discrete spectrum levels in the energy range below the middle of the bandgap. However, the energy of states formed from the Bloch functions of the conduction band with the dispersion relation (18) cannot be less than  $-E_g/2$ . Moreover, this value is reached at the minimum of the subband at  $k_{\parallel} = 0$  and the energy level  $k_z^2/2m^* = -E_g/4$ . More negative values of the level energy are impossible, since in this case the radical expression would become negative, an imaginary component would appear in the energy, and such a state cannot be stationary.

Thus, states with energies from the lower half of the bandgap can only be formed from the Bloch functions of the valence band, when the relationship between the energy  $E$  and the quasimomentum components ( $k_{\parallel}, k_z$ ) will be determined by the second root  $E_v$  (19) of the dispersion equation (17). Such an effective mass equation for the nonparabolic valence band within the two-band Kane model can be obtained from the system of equations (4.13) of the work [4] in exactly the same way as the effective mass

equation for the conduction band (15). This equation will have the same form as (15) with an accuracy to small smoothness corrections proportional to the derivatives of the potential  $\partial U/\partial z$  of different orders. Only its eigenvalues  $E$  must belong to the spectrum region  $E < -E_g/2$  due to the aforementioned restrictions on the radical expression.

However, this equation has the drawback of associating negative kinetic energy with the  $|E\rangle$  state. Since all standard equations of mathematical physics describe the dynamics of free particles with positive kinetic energy, the direct application of such an effective mass equation will give solutions that oscillate in the sub-barrier region and decay in the over-barrier region. It is impossible to search for wave functions of discrete states in this form.

It is possible to proceed to the eigenfunctions and spectrum of the time-reversed problem as a solution to this problem. In our case, due to the real nature of the original single-particle Hamiltonian in Kane's theory and the eigenfunctions of the half-space problem, this will amount to only changing the sign of the eigenvalue  $E' = -E$  and the roots of the dispersion equation. If they are renumbered in descending order of energy from top to bottom, then  $E'_1(k^2) = -E_v(k^2), E'_2(k^2) = -E_c(k^2)$ . The zero of the energy scale is still defined by the condition that the electrostatic potential vanishes at infinity, corresponding

to the edge of the continuous spectrum of the former conduction band, which will take the place of the valence band in this representation. The valence band moves to the place of the conduction band with the upper limit of the bandgap at  $E' = E_g$ . The solution of the Poisson equation and the electrostatic energy do not change.

In fact, with such a transformation, the matter reduces to replacing  $E \rightarrow -E'$  in the quasipotential and searching for discrete eigenvalues in the range  $E_g/2 < E' < E_g$ . It is evident that under this transformation, the term linear in  $U$  in the effective mass equation becomes repulsive instead of attracting to the surface. Nevertheless, the term quadratic in  $U$  can still create a potential well in this case also. Thus, one may hope, the issue of the existence of two-dimensional valence subbands in the accumulation layer on the surface of an  $n$ -type semiconductor becomes a question of numerical relationships between parameters rather than a fundamental one. In agreement with Keldysh's remark.

If two-dimensional subbands with a positive effective mass are found, the obtained spectrum should be multiplied by  $-1$  upon reverting to the original space. The resulting valence-type states in the bandgap should be occupied with electrons and contribute to the total density of quasi-two-dimensional electrons in the accumulation layer, as they lie below the Fermi level located in the conduction band. It should be noted that transport along such subbands on the surface is expected to be of the hole type due to the negative dynamic mass  $1/m_v^* = (\partial E_v / \partial k_{\parallel}) / k_{\parallel}$ .

As possible experimental evidence in favor of the existence of two-dimensional valence subbands in the potential well for electrons, one might consider the gate voltage  $V_g$  dependencies of the occupation of subbands in the accumulation layer and inversion channel on the silicon surface in the MOSFET structure (see Figure 1 and Figure 3 in the article [24]). In both cases, the threshold nature of the increase in the number of electrons in the newly appeared subband with rising gate voltage is clearly observed. However, in the case of an accumulation layer, the threshold nature of the deepening of the subband near the boundary with a continuous spectrum appears natural. The threshold behavior observed in the inversion channel, if assumed as to be formed by a two-dimensional conduction subband, cannot be explained. Since such a subband would have been detached from the boundary of the continuous conduction band spectrum long before reaching the top of the valence band. On the other hand, the threshold occupation of the newly formed valence subband in the bandgap by electrons is quite expected.

## 4. Conclusion

The conducted research showed the opportunity of using threshold theory formulas to evaluate shallow binding states, even if these states are not the ground states in a given potential well, but are excited states that do not

conform to the commonly accepted conditions for the existence of threshold phenomena. Amendments to the threshold formulas were obtained, which expand the range of applicability of the basic relations. Signatures of the possible existence of two-dimensional valence subbands in the energy spectrum of the accumulation layer on the surface of  $n$ -type semiconductor were identified.

The results presented here did not confirm the hypothesis regarding the existence of „kinetically bound“ states, proposed in [2] and supported in [9]. The emergence of this hypothesis is associated with an attempt to explain the observed threshold nature of the dependence of subband energies on gate potential. The material in this paper shows that threshold behavior occurs without the assumption of the existence of two-dimensional subbands, whose spectrum starts with  $k_{\parallel} \neq 0$ .

Finally, it should be noted that the analysis of threshold behavior can have not only a purely practical value, as a method for more accurately determining the moment of the appearance of a new subband, but also serve as a means of investigating whether it belongs to the conduction band or valence band.

## Conflict of interest

The authors declare that they have no conflict of interest.

## References

- [1] V.F. Radantsev, T.I. Deryabina, L.P. Zverev, G.I. Kulaev, S.S. Khomutova. *ZhETF* **91**, 1029 (1986). (in Russian).
- [2] R.E. Doezema, H.D. Drew *Phys. Rev. Lett.* **57**, 762 (1986).
- [3] A.I. Baz, Ya.B. Zeldovich, A.M. Perelomov. *Rasseynaniye, reaktsii i raspady v nerelativistskoy kvantovoy mekhanike. 2 izd.* Nauka, M. (in Russian). (1971).
- [4] A.Ya. Shulman, D.V. Posvyansky. *ZhETF*, **157**, 6, 1072 (2020). (in Russian).
- [5] D.V. Posvyansky, A.Ya. Shulman. *ZhETF* **136**, 1, 169 (2009). (in Russian).
- [6] Yu.L. Balkarey, V.B. Sandrmirsky. *ZhETF* **54**, 3, 808 (1968). (in Russian).
- [7] V.F. Radantsev, V.V. Kruzhaev. *Int. J. Nanosci.* **06**, 301 (2007).
- [8] Kyoung-Youm Kim, Byoung-ho Lee. *IEEE J. Quantum Electron.* **37**, 546 (2001).
- [9] M. Kubisa, W. Zawadzki. Kinetic confinement of electrons in modulated semiconductor structures. In: *From Quantum Mechanics to Technology. Lecture Notes in Physics.* Z. Petru, J. Przystawa, K. Rapcewicz. /EDS V. 477. Springer, Berlin (1996).
- [10] V.M. Galitsky, V.M. Karnakov, V.I. Kogan. *Zadachi po kvantovoy mekhanike. 2-e izd.* Nauka, M. (1992). 880 s. (in Russian).
- [11] H. Bethe, R. Peierls. *Proc. Royal Soc. A* **148**, 146 (1935).
- [12] E.P. Wigner. *Phys. Rev.* **73**, 1002 (1948).
- [13] A.Ya. Shulman, D.V. Posvyansky. *Tezisy XIV Ros konf. po fizike poluprovodnikov.* Novosibirsk (2019). 253 s. (in Russian).
- [14] V.V. Stepanov. *Kurs differentsial'nykh uravneniy.* 8-e izd. GIFML, M. (1959). Gl. VI, § 2.4. (in Russian).

- [15] A.Ya. Shulman. Funktsional'nyy podkhod k beskonechnym sistemam s neodnorodnym elektronnyim gazom. Matematicheskii apparat. In preparation.
- [16] L.D. Landau, E.M. Lifshitz. Kvantovaya mekhanika. Nauka, M. (1989). 768 s. (in Russian).
- [17] O.V. Konstantinov, A.Ya. Shik. ZhETF **58**, 5, 1662 (1970). (in Russian).
- [18] A.Ya. Shulman. Uravneniye effektivnoy massy dlya poluprovodnika s neparabolicheskoy zonoy provodimosti. Tezisy XXIV Ural'skoy mezhdunar. zimney shk. po fizike poluprovodnikov. Ekaterinburg (2022). S. 145. (in Russian).
- [19] H. Reisinger, H. Schaber, R.E. Doezema. Phys. Rev. **B 24**, 5690 (1981).
- [20] A. Zhang, J. Slinkman, R.E. Doezema. Phys. Rev. **B 44**, 10752 (1991).
- [21] F. Stern. J. Computat. Phys. **6**, 56 (1970).
- [22] A.Ya. Shul'man. J. Phys.: Conf. Ser. **35**, 163 (2006).
- [23] L.V. Keldysh. ZhETF **45**, 2, 364 (1963). (in Russian).
- [24] G.M. Gusev, Z.D. Kvon, V.N. Ovsyuk. Solid State Commun. **49**, 9, 899 (1984).

*Translated by E.Potapova*